

## Lattice Dynamical Study of Indium Pnictides (In P, InAs, InSb)

\*Suresh Chandra Pandey<sup>1</sup>, Kripa Shankar Upadhyaya<sup>2</sup>, Bharat Mishra<sup>3</sup>

<sup>1</sup>Department of Physics, Mahatma Gandhi Gramodaya Vishwavidyalaya, Chitrakoot, Satna M.P., India

<sup>2</sup>Department of Physics, Nehru Gram Bharati University, Allahabad, U.P., India

<sup>3</sup>Department of Physics, Mahtma Gandhi Gramodaya Vishwavidyalaya, Chitrakoot, Satna M.P., India

Corresponding Author: Suresh Chandra Pandey

**Abstract:** The compound lattice dynamics (phonon dispersion curves, Debye temperatures variation, combined density of states (CDS) curves, two-phonon Raman and anharmonic elastic properties) of InP, InAs, InSb with zinc-blende structure has been investigated including van der Waal's three-body force shell model (VTSM). This model incorporates the effect of van der Waal's interactions and three-body interactions into the rigid shell model of zinc blende structure, where the short range interactions are operative upto the second neighbours. Our results are in good agreement with the available measured data. It is concluded that this model VTSM will be equally applicable to study above properties of other zinc-blende structure solids as compared to the models of earlier workers.

**Keywords:** Phonons, van der Waal's interactions, Debye temperatures variation, Combined density of states curve, Raman spectra, Phonon dispersion curves, Lattice dynamics, InP, InAs, InSb.

Date of Submission: 28-08-2017

Date of acceptance: 13-09-2017

### I. Introduction

Structurally, the most semiconductors consist of a network of covalent bonds leading to an open crystal structure. The general theory of lattice dynamical model, [1, 2] in the specific case discussed for phonon dispersion curves for various II-VI and III-V compounds exhibit tetra hedral coordination under ambient conditions. In this communication we are mainly concerned with lattice dynamical study of Pnictides (InP, InAs, InSb), the experimental data for phonon dispersion curves of InP [3, 4], InAs [5, 6] InSb [7], harmonic and anharmonic elastic constants [8, 9, 10], Debye temperature variation [11, 12, 13, 14, 15, 16] and Raman spectra [17] for InP, [18] for InAs, two phonon IR spectra [22, 23] for InSb are available. Further more, effect of long range (LR) three body interactions (TBI), short range interaction Vander Waal's (VDW) attractions are significant, in partially ionic and covalent crystals [24]. Though, van der Waal's interactions have much effective force, but Singh and Singh [25] have used only three body force shell model (TSM) formulation for InP, InAs, and InSb without inclusion of van der Waal's interaction (VDWI). So far, the calculations on third order elastic constants (TOEC) and pressure derivative of second order elastic constant (SOEC) are concerned, Sharma and Verma [26] have reformulated the expressions derived by Garg et.al. [27]. They have derived the correct expression for TOEC and pressure derivatives of SOEC for ZBS Crystals. The various coresearchers Upadhyay et.at. [28, 29], Tiwari et. at. [30], Srivastava and Upadhyaya [31], Mishra and Upadhyaya [32], Dubey et. at. [33, 34], Pandey et. al. [35] used their correct expression for calculating the anharmonic elastic properties for NaCl, CsCe and ZBS structure of solids. Therefore we have used expressions of Sharma and Verma [26] as such for our computations.

### II. Theoretical Framework Of The Present Model

We have developed a model for ZBS structure, which includes the effect of van der Waal's interactions (VDWI) and three body interactions (TBI) in the frame work of rigid shell model (RSM) where short range interactions are effective upto the second neighbours and known as van der Waal's three body force shell model (VTSM).

#### 2.1. Secular equations:

For ZBS crystals, the cohesive energy for a particular lattice separation ( $r$ ) has been expressed as

$$\Phi(r) = \Phi_{LR}(r) + \Phi_{SR}(r) \quad (1)$$

where the first term  $\Phi_{LR}(r)$  represent the long-range Coulomb and three body interaction (TBI) energies expressed by

$$\Phi_{LR}(r) = - \sum_{\substack{ij \\ i \neq j \neq k}} \frac{Z_i Z_j e^2}{r_{ij}} \left\{ 1 + \sum_k f(r_{ik}) \right\} = - \frac{\alpha_M Z^2 e^2}{r} \left\{ 1 + \frac{4}{Z} f(r) \right\} \quad (2)$$

where  $Z_i$  is the ionic charge parameter of  $i^{th}$  ion,  $r_{ij}$  separation between  $i^{th}$  and  $j^{th}$  ion,  $f(r_{ik})$  is the three-body force parameter dependent on nearest-neighbour separation  $r_{ik}$  and is a measure of ion size difference Singh [24],  $\alpha_M$  is Madelung constant (=1.63805 for ZBS).

The second term in equation (1) is short-range energy contributions from overlap repulsion and van der Waals interactions (VDWI) expressed as [60].

$$\Phi_{SR}(r) = Nb \sum_{i,j=1}^2 \exp \left[ \frac{r_i + r_j - r_{ij}}{\rho} \right] - \sum_{ij} \frac{c_{ij}}{r_{ij}^6} - \sum_{ij} \frac{d_{ij}}{r_{ij}^8} \quad (3)$$

where  $N$  is the Avogadro's a number,  $b$  is the hardness parameter and the first term is the Hafemeister and Flygare (HF) potential [31] and used by Singh and coworkers. The second term and third term represent the energy due to VDW for  $c_{ij}$  dipole-dipole (d - d) and  $d_{ij}$  dipole - quadrupole (d - q) interactions, respectively.

Using the crystal energy expression (1), the equations of motion of two cores and two shells can be written as;

$$\omega^2 \underline{M} \underline{U} = (\underline{R} + \underline{Z}_m \underline{C}' \underline{Z}_m) \underline{U} + (\underline{T} + \underline{Z}_m \underline{C}' \underline{Y}_m) \underline{W} \quad (4)$$

$$0 = (\underline{T}^T + \underline{Y}_m \underline{C}' \underline{Z}_m) \underline{U} + (\underline{S} + \underline{K} + \underline{Z}_m \underline{C}' \underline{Y}_m) \underline{W} \quad (5)$$

Here  $\underline{U}$  and  $\underline{W}$  are vectors describing the ionic displacements and deformations, respectively.  $\underline{Z}_m$  and  $\underline{Y}_m$  are diagonal matrices of modified ionic charges and shell charges, respectively;  $\underline{M}$  is the mass of the core;  $\underline{T}$  and  $\underline{R}$  are repulsive Coulombian matrices respectively;  $\underline{C}'$  are long-range interaction matrices that include Coulombian and TBI;  $\underline{S}$  and  $\underline{K}$  are core-shell and shell-shell repulsive interaction matrices, respectively and  $\underline{T}^T$  is the transpose of matrix  $\underline{T}$ . The elements of matrix  $\underline{Z}_m$  consist of the parameter  $Z_m$  giving the modified ionic charge.

$$Z_m = \pm Z \sqrt{1 + \left( \frac{8}{Z} \right) f(r_0)} \quad (6)$$

The elimination of  $\underline{W}$  from eqns. (4) and (5) leads to the secular determinant;

$$\left| \underline{D}(\bar{q}) - \omega^2 \underline{M} \underline{I} \right| = 0 \quad (7)$$

for the frequency determination. Here  $\underline{D}(\bar{q})$  is the  $(6 \times 6)$  dynamical matrix given by

$$\underline{D}(\bar{q}) = (\underline{R} + \underline{Z}_m \underline{C}' \underline{Z}_m) - (\underline{T} + \underline{Z}_m \underline{C}' \underline{Y}_m) \times (\underline{S} + \underline{K} + \underline{Y}_m \underline{C}' \underline{Y}_m)^{-1} (\underline{T}^T + \underline{Y}_m \underline{C}' \underline{Z}_m) \quad (8)$$

The numbers of adjustable parameters have been largely reduced by considering all the short-range interactions to act only through the shells.

## 2.2. Vibrational Properties of Zinc-Blende Structure:

By solving the secular equation (4) along  $[q \ 0 \ 0]$  direction and subjecting the short and long-range coupling coefficients to the long-wavelength limit  $\bar{q} \rightarrow 0$ , two distinct optical vibration frequencies are obtained as

$$(\mu \omega_L^2)_{q=0} = R'_0 + \frac{(Z'e)^2}{vfL} \cdot \frac{8\pi}{3} (Z_m^2 + 4Zr_0 f'(r_0)) \quad (9)$$

$$(\mu \omega_T^2)_{q=0} = R'_0 - \frac{(Z'e)^2}{vfT} \cdot \frac{4\pi}{3} Z_m^2 \quad (10)$$

where the abbreviations stand for

$$R'_0 = R_0 - e^2 \left( \frac{d_1^2}{\alpha_1} + \frac{d_2^2}{\alpha_2} \right); R_0 = \frac{e^2}{v} \left[ 4 \frac{A_{12} + 2B_{12}}{3} \right]; Z' = Z_m + d_1 - d_2 \quad (11)$$

$$f_L = 1 + \left( \frac{\alpha_1 + \alpha_2}{v} \right) \cdot \frac{8\pi}{3} (Z_m^2 + 4Zr_0 f'(r_0)) \quad (12)$$

$$f_T = 1 - \left( \frac{\alpha_1 + \alpha_2}{v} \right) \cdot \frac{4\pi}{3} \tag{13}$$

and

$$\alpha = \alpha_1 + \alpha_2 \tag{14}$$

and  $v = 3.08r_0^3$  for ZBS (volume of unit cell).

**2.3. Debye Temperatures Variation:**

The specific heat at constant volume  $C_v$  at temperature  $T$  is expressed as

$$C_v = 3NK_B \frac{\int_0^{v_m} \left\{ \left( \frac{hv}{K_B T} \right)^2 e^{hv/K_B T} \right\} G(v) dv}{\int_0^{v_m} G(v) dv} / (e^{hv/K_B T} - 1)^2 \tag{15}$$

where,  $v_m$  is the maximum frequency,  $h$  is the Planck's constant and  $K_B$  is the Boltzmann's constant. The equation (15) can be written as a suitable form for a computational purpose as

$$C_v = 3NK_B \frac{\sum_v \{E(x)\} G(v) dv}{\sum_v G(v) dv} \tag{16}$$

where  $E(x)$  is the Einstein function, defined by

$$E(x) = x^2 \frac{\exp(x)}{\{\exp(x) - 1\}^2} \tag{17}$$

where  $x = \left\{ \left( \frac{hv}{K_B T} \right)^2 e^{\frac{hv}{K_B T}} \right\}$

Also,  $\sum_v G(v) dv =$  Total number of frequencies considered.  
 $= 6000$  for zinc-blende structure.

Hence, equation (16) can be written for zinc-blende structure type crystals, as

$$C_v = \frac{3NK_B}{6000} \sum_v E(x) G(v) dv \tag{18}$$

The contribution of each interval to the specific heat is obtained by multiplying an Einstein function corresponding to mid-point of each interval (say 0.1 THz) by its statistical weight. The statistical weight of the interval is obtained from the number of frequencies lying in that interval. The contributions of all such intervals, when summed up give,  $\sum_v E(x) G(v) dv$ . The Specific heat  $C_v$  is then calculated by expression (18).

**2.4. Second and third order elastic constants:**

Proceeding with the use of three body crystal potential given by equation (1), (Sharma and Verma [26]) have derived the expressions for the second order elastic constants and used by (Singh and Singh [25]) for zinc-blende structure crystals. We are reporting them here as their corrected expressions.

The expressions for second order elastic constants (SOEC) are-

$$C_{11} = L \left[ 0.2477 Z_m^2 + \frac{1}{3} (A_1 + 2 B_1) + \frac{1}{2} (A_2 + B_2) + 5.8243 Z a f'(r_0) \right] \tag{19}$$

$$C_{12} = L \left[ -2.6458 Z_m^2 + \frac{1}{3} (A_1 - 4 B_1) + \frac{1}{4} (A_2 - 5 B_2) + 5.8243 Z a f'(r_0) \right] \tag{20}$$

$$C_{44} = L \left[ -0.123 Z_m^2 + \frac{1}{3} (A_1 + 2 B_1) + \frac{1}{4} (A_2 + 3 B_2) - \frac{1}{3} \nabla (-7.539122 Z_m^2) + A_1 - B_1 \right] \tag{21}$$

where  $A_1 = A_{12}, B_1 = B_{12}, A_2 = A_{11} + A_{22}, B_2 = B_{11} + B_{22}, C_1 = \frac{A_{12}^2}{B_{12}}$  and  $C_2 = \frac{A_2^2}{B_2}$

and the expressions for third order elastic constants (TOEC) are-

$$C_{111} = L \left[ \begin{array}{l} 0.5184Z_m^2 + \frac{1}{9}(C_1 - 6B_1 - 3A_1) + \frac{1}{4}(C_2 - B_2 - 3A_2) - 2(B_1 + B_2) - \\ 9.9326Zaf'(r_0) + 2.5220Za^2f''(r_0) \end{array} \right] \quad (22)$$

$$C_{112} = L \left[ \begin{array}{l} 0.3828Z_m^2 + \frac{1}{9}(C_1 + 3B_1 - 3A_1) + \frac{1}{8}(C_2 + 3B_2 - 3A_2) - 11.642Zaf'(r_0) + \\ 2.5220Za^2f''(r_0) \end{array} \right] \quad (23)$$

$$C_{113} = L \left[ \begin{array}{l} 6.1585Z_m^2 + \frac{1}{9}(C_1 + 3B_1 - 3A_1) - 12.5060Zaf'(r_0) + 2.5220Za^2f''(r_0) \end{array} \right] \quad (24)$$

$$C_{144} = L \left[ \begin{array}{l} 6.1585Z_m^2 + \frac{1}{9}(C_1 + 3B_1 - 3A_1) - 4.1681Zaf'(r_0) + 0.8407Za^2f''(r_0) + \\ \nabla \left\{ -3.3507Z_m^2 - \frac{2}{9}C_1 + 13.5486af'(r_0) - 1.681a^2f''(r_0) \right\} + \\ \nabla^2 \left\{ -1.5637Z_m^2 + \frac{2}{3}(A_1 - B_1) + \frac{C_1}{9} - 5.3138Zaf'(r_0) + 2.9350Za^2f''(r_0) \right\} \end{array} \right] \quad (25)$$

$$C_{166} = L \left[ \begin{array}{l} -2.1392Z_m^2 + \frac{1}{9}(C_1 - 6B_1 - 3A_1) + \frac{1}{8}(C_2 - 5B_2 - 3A_2) - (B_1 + B_2) - \\ 4.1681Zaf'(r_0) + 0.8407Za^2f''(r_0) + \\ \nabla \left\{ -8.3768Z_m^2 + \frac{2}{3}(A_1 - B_1) - \frac{2}{9}C_1 + 13.5486af'(r_0) - 1.681a^2f''(r_0) \right\} + \\ \nabla^2 \left\{ 2.3527Z_m^2 + \frac{1}{9}C_1 - 5.3138Zaf'(r_0) + 2.9350Za^2f''(r_0) \right\} \end{array} \right] \quad (26)$$

$$C_{456} = L \left[ \begin{array}{l} 4.897Z_m^2 + \frac{1}{9}(C_1 - 6B_1 - 3A_1) - B_2 + \\ \nabla \left\{ -5.0261Z_m^2 - \frac{1}{9}C_1 \right\} + \nabla^2 \left\{ 7.0580Z_m^2 + \frac{1}{3}C_1 \right\} + \\ \nabla^3 \left\{ -4.8008Z_m^2 + \frac{1}{3}(A_1 - B_1) - \frac{1}{9}C_1 \right\} \end{array} \right] \quad (27)$$

where  $Z_m$  is the modified ionic charge defined earlier with  $L = \frac{e^2}{4a^4}$  and

$$\nabla = \left[ \begin{array}{l} -7.53912Z(Z + 8f(r_0)) + (A_1 - B_1) \\ -3.141Z(Z + 8f(r_0)) + (A_1 + 2B_1) + 21.765Zaf'(r_0) \end{array} \right] \quad (28)$$

and Pressure derivatives of SOEC

$$\frac{dK'}{dP} = -(3\Omega)^{-1} \left[ \begin{array}{l} 20.1788Z_m^2 + 3(A_1 + A_2) + 4(B_1 + B_2) + (C_1 + C_2) - 104.8433Zaf'(r_0) \\ + 22.7008Za^2f''(r_0) \end{array} \right] \quad (29)$$

$$\frac{dS'}{dP} = -(2\Omega)^{-1} \left[ \begin{array}{l} -11.5756Z_m^2 + 2(A_1 - 2B_1 + \frac{3A_2}{2} - \frac{7B_2}{2} + \frac{1}{4} \cdot C_2 + \dots) \\ 37.5220Zaf'(r_0) \end{array} \right] \quad (30)$$

$$\begin{aligned} \frac{dC'_{44}}{dP} = &-(\Omega)^{-1} \left[ \left\{ 0.4952Z_m^2 + \frac{1}{3}(A_1 - 4B_1 + C_1) + \frac{1}{2} \cdot A_2 - \frac{3}{2} \cdot B_2 + \frac{1}{4} \cdot C_2 + 4.9667Zaf'(r_0) \right. \right. \\ &+ 2.522Za^2 f''(r_0) \left. \right\} \\ &+ \nabla \left\{ -17.5913Z_m^2 + A_1 - B_1 - \frac{2}{3} \cdot C_1 + 40.6461Zaf'(r_0) + 5.044Za^2 f''(r_0) \right\} \\ &+ \nabla^2 \left\{ 3.1416Z_m^2 + \frac{2}{3}(A_1 - B_1) + \frac{1}{3} \cdot C_1 - 15.9412Zaf'(r_0) \right. \\ &\left. \left. + 8.8052Za^2 f''(r_0) \right\} \right] \quad (31) \end{aligned}$$

where  $K = \frac{C_{11} + 2C_{12}}{3}$ ,  $S = \frac{C_{11} - C_{22}}{2}$

and  $\Omega = -5.0440Z_m^2 + (A_1 + A_2) - 2(B_1 + B_2) + 17.4730Zaf'(r_0)$

The values of  $A_i, B_i$  and  $C_i$  as defined by Sharma and Verma [21].

### III. Computations

The value of input data [3, 5, 7, 37, 38, 39, 40, 42, 43, 44, 46] for indium pnictides (InP, InAs, InSb) and model parameters have been shown in Table 1. The values of  $A_i, B_i, C_i$  have been calculated from the knowledge of  $b, \rho$ ; the value of various order of derivatives of  $f(r_0)$  and van der Waal's coupling coefficient [26] the value of VDW coefficient used by us in the present study have been determined using the Slatre-Kirkwood variation (SKV) method [47], Lee [48] approach as suggested by Singh and Singh [25] and reported by Sharma and Verma [26]. Thus our model parameters are ( $b, \rho, f(r_0), r_0 f'(r_0), A_{12}, A_{11}, A_{22}, B_{12}, B_{11}, B_{22}, d_1, d_2, Y_1$  and  $Y_2$ ). The values of the van der Waal's coefficients (VDW) are shown in Table 2. Our model parameters of VTSM have been used to compute the phonon spectra of InP, InAs, InSb for the allowed 48 non equivalent wave vector in the first Brillouin zone. The frequencies along the symmetry directions have been plotted against the wave vector to obtain the phonon dispersion curves (PDCs). These curves have been compared with those measured by means of the coherent inelastic neutron scattering technique [3, 4] in Fig. 1 along with the BBFM calculations of Kunc. et al. [37]. Since the neutron scattering experiments provide us only very little data for symmetry directions for InP. Phonon dispersion curves of InAs have been compared with those measured by means of the coherent in elastic neutron scattering technique, thermal diffuse X-ray data [17] in figure 2 along with OVSM calculation of Borchers and Kunc [6]. Phonon dispersion curves (PDC) of InSb compared with measured by coherent inelastic neutron scattering technique [7] especially TA modes are very much different not only from ours but from BCM calculations of Rajput and Broun [49] alongwith in figure 3. Since the neutron scattering provide us only very little data for symmetry directions we have also computed combined density of state (CDS) and Debye temperature variation for the complete description of the frequencies of Brillouin zone.

The complete phonon spectra have been used to compute the combined density of states (CDS),  $N(v_j + v'_j)$  corresponding to the sum modes ( $v_j + v'_j$ ) following procedure of Smart et.al. [50]. A histogram between  $N(v_j + v'_j)$  and  $(v_j + v'_j)$  have been plotted and smoothed out as shown in fig. 2(a), 2(b) and 2(c). These curves show well defined peaks which correspond to two phonon Raman scattering for InP, InAs and two phonon IR spectra for InSb. These CDS peaks have been compared with the assignments calculated and shown in table 3, table 4 and table 5.

The Debye temperature variation VTSM for InP[11], InAs [11, 12, 13] and InSb [11, 12, 14, 15, 16] and those calculated by us using VTSM has been compared in fig. 7, fig. 8 and fig. 9. The calculated value of TOEC using equations (22-27) have been compared with calculated values of Sadao Adachi [51] and shown in table 4. The pressure derivatives of SOEC also have been calculated and compared with those measured by Wolf Ger lich [52] for InP, Soma et. al. [54] for InAs and by Persada [55] have also been calculated us compared with these calculated by ford et. al. [53] in table 5.

#### **IV. Results And Discussion**

From figure 1. our phonon dispersion curves for InP agree well with measured data reported by Borchers et. al. [3]. It is evident from PDCs that our predictions using present model (VTSM) are better than those by using BBFM [37]. Our model has successfully explained the dispersion of phonons along the three symmetry directions from fig. 1 and table 8. Our model has 21.21% improvement over BBFM from fig 2. Our phonon dispersion curve for InAs agree well with measured Raman data reported by Carles et. al. [5]. It is evident from PDCs that our prediction using present model (VTSM) are better than those by using OVSM [6]. from table 9 our model has 17.72% Improvement over OVSM. The phonon dispersion curves for InSb agree well with measured data reported by Price et. al. [7]. It is evident from PDCs that our predictions using present model (VTSM) are better than those by using BCM [49]. Our model has successfully explained the dispersion of phonons along the three high symmetric directions from fig. 3 and table 10. It is clear that our model has 5.26% along LO(X), 5.36% along TA(X) and 5.10% along TA(L) improvement over BCM due to inclusion of TBI and VDWI coefficients. Thus, our VTSM model has better agreement with experimental data over BCM [49].

#### **Combined density of State:**

The present model is capable to predict the two phonon Raman spectra [20] for InP, two phonon Raman spectra [21] for InAs, and two phonon IR spectra [22, 23], the results of these investigations for CDSs peak have been presented in fig. 4, fig. 5 and fig. 6. The theoretical peaks are in good agreement with both observed Raman spectra of InP, InAs and IR spectra for InSb, the assignments made by the critical point analysis have been shown in table 3, table 4 and table 5. The interpretations of spectra achieved from both CDS approach and critical point analysis is quite satisfactory. This explains that there is an excellent agreement between experimental data and our theoretical results.

#### **Third order elastic constants (TOEC) and pressure derivatives of second order elastic constants (SOEC):**

Our calculations on TOEC of InP, InAs and InSb compared with the theoretical results of Sadao adachi [51] as shown in table 6. Further, pressure derivatives of SOEC for InP, InAs and InSb have also been compared with the measured data of [52-55] as shown in table 7. The results in are good agreement.

#### **Debye temperature variation:**

From fig. 7, 8 and 9, our study shows a better agreement with measured data of [11-19] and theoretical results of BBFM [37] for InP, VFFM [56] for InAs and BCM [49] for InSb. We can say that our present model gives a better interpretation of the Debye temperature variation for Indium Pnictides.

#### **V. Conclusion**

The inclusion of van der waal's interaction (VDWI) with TBI have influenced both the optical branches and the acoustic branches. Another striking feature of present model is noteworthy from excellent reproduction of almost all branches of PDCs. Hence the prediction of phonon dispersion curves (PDC) for Indium Pnictides using VTSM may be considered more satisfactory than from other models BBFM [37], VFFM [56] and BCM [49]. The basic aim of the study of two phonon raman and two phonon IR spectra is to correlate the neutron scattering and optical measured data of InP, InAs and InSb. In this paper, we have systematically reported phonon dispersion, curves, combined density of states, Debye temperature variation and a part of harmonic and anharmonic properties of InP, InAs and InSb. On the basis of overall discussion it is concluded that our van der Waal's three body force shell model (VTSM) is adequately capable of describing the crystal dynamics of indium pnictides (InP, InAs, InSb). Our work gets strong support from paper of Mishra and Upadhyay [32] and Dubey et. al. [33, 34].

#### **Acknowledgements**

The authors are thankful to computer centre B.H.U. Varanasi, India for providing computational assistance. One of us Suresh Chandra Pandey is grateful to Dr. Uma Shankar Mishra Mahatma Gandhi Gramodaya Viswavidyalaya, Chitrakoot, Satna M.P., India for encouragement, and also thankful to Dr. K.K. Mishra, Professor in department of physics, Lingaya's University Faridabad, India for many useful discussions.

#### **References**

- [1]. Born M. and Huang K., Dynamical Theory of Crystal Lattices, Oxford University Press 1954.
- [2]. Maradudin A. A., Montroll E. and Weiss J., Theory of Lattice Dynamics in the Harmonic Approximation, Supplement 3, Solid State Physics, Academic Press, New York (1963-1964).
- [3]. Borchers P.H., Alfrey G., Sauderson D.H. and Wood A.D.B., (1975) Phys. C 8, 2022.
- [4]. Ram R.K., Kushwaha M.S. and Shukla A., (1989) Phys. Stat. Solidi B 154, 553.
- [5]. Carles, R., Saint-Cricq, N., Renucci, J.B., Renucci, M.A. Zwik, A. : (1980) Phys. Rev. B22, 4804.

[6]. P.H. Borchers and K. Kunc, (1978) J. Phys. C11, 4145.  
 [7]. Price D.L., Rowe J.M. and Nicolow R.M., (1971) Phys. Rev., B3, 1268.  
 [8]. Kunc K., Balkanski M. and Nusimovici M. A., (1975) Phys. Status Solidi (b) 72, 229.  
 [9]. Gray, D.W. (1972), American Institute of Physics hand book. 3<sup>rd</sup> ed.  
 [10]. Slutsky J. and Garland, C. W., (1959) Phys. Rev. 113, 167.  
 [11]. U. Piesbergen, (1966) Semiconductors and Semimetals 2, 49.  
 [12]. T.C. Cetas, C.R. Tilford, and C.A. Swenson, (1968) Phys. Rev. 174, 835.  
 [13]. N. N. Sirota, A.M. Antyukhov, V.V. Novikov, V.A. Fyodorov, (1982) Cryst. Res. Technol. 17, 279.  
 [14]. Gulyaev P. V. and Petrov A. V., (1959) Sov. Phys. Sol. Stat. 1, 330.  
 [15]. Banerjee R. and Varshni Y. P., (1969) Canad. J. Phys., 47, 451.  
 [16]. Passler S. R., (2013) AIP Advances 3, 082108.  
 [17]. Orlova, N.S. : (1983) Phys. Status Solidi (b) 119, 541.  
 [18]. Talwar D. N. and Agrawal B.K., (1972) Phy. Rev. B8, 693.  
 [19]. Talwar D. N. and Agrawal B.K., (1972) Solid State Comm., 11, 1691.  
 [20]. Alfray G. F. and Borchers P. H., (1972) J. Phys. C 5, 1275.  
 [21]. M. Cardona, in light scattering in solids, topics in applied physics, edited by M.Cardona (Springer, Berlin 1976) vol 8, P.I.  
 [22]. Koteles E. S. and Datars W.R., (1974) Phys. Rev. B 9, 572.  
 [23]. Fray S. J., Johnson F. A. and Jones R. Proc., (1960) Phys. Soc. London, 76, 939.  
 [24]. Singh, R. K., (1982) Physics Reports (Netherlands), 85, 259.  
 [25]. Singh, R. K., Singh, S., (1987) Phys. Status Solidi (b) 140, 407.  
 [26]. Sharma, U.C. and Verma, M. P., (1980) Phys. Status Solidi (b) 102, 487.  
 [27]. Garg V.K., Puri D. S., Verma M. P., (1978) Phys. Status Solidi (b) 87, 401.  
 [28]. Upadhyaya, K. S., Pandey, A, Srivastava, D.M. Chinese J., (2006) Phys. 44, 127.  
 [29]. Upadhyaya, K. S., Upadhyay, G.K., Yadav, M., Singh, A.K., (2001) J. Phys. Soc. Japan, 70, 723.  
 [30]. Tiwari, S. K., Pandey, L. K., Shukla, L. J., Upadhyaya, K. S., (2009) Physica Scr., 80, 065603.  
 [31]. Srivastava, U.C., Upadhyaya, K.S., (2011) Physical Rev. and Res. Int., 1, 16.  
 [32]. Mishra, K.K., Upadhyaya, K.S., (2012) Int., Jour. Sci. Engg. Res., 3, 1388.  
 [33]. Dubey J.P., Tiwari R.K., Upadhyaya K.S. and Pandey P.K., (2015) Turk. J. Phys. 39, 242.  
 [34]. Dubey J.P., Tiwari R.K., Upadhyaya K.S. and Pandey P.K., (2015) Jour. Of Appl. Phys. (IOSR-JAP) 7, 67.  
 [35]. Pandey S.C., Dubey J.P. and Upadhyaya K.S., (2016) Jour. Of Appl. Phys. 8, 01.  
 [36]. Tolpygo K.B., (1961) Sov.Phys.Solid State,3,98.  
 [37]. Kunc K., Balkanski M. and Nusimovici M.A., (1975) Phys. Status Solidi (b) 72, 229.  
 [38]. Gray, D.W. (1972), American Institute of Physics hand book. 3<sup>rd</sup> ed.  
 [39]. Kushwaha M.S. and Kushwaha S.S., (1980) cand J. Phys. 58, 351  
 [40]. Levinstein M, Rumyantsev S and Shur M, (1990) hand book series on semiconductor parameters vol 1, 2 (London : world scientific)  
 [41]. M. Cardona, in light scattering in solids, topics in applied physics, edited by M.Cardona (Springer, Berlin 1976) vol 8, P.I.  
 [42]. Shankar, J., Sharma, J.C., Sharma, D.P., (1977) Ind. Jour. Pure Appl. Phys., 15, 811.  
 [43]. Slutsky J. and Garland, C.W., (1959) Phys. Rev. 113, 167.  
 [44]. Banerjee R. and Varshni Y.P., (1969) Canad. J. Phys., 47, 451.  
 [45]. Kunc K., Balkanski M. and Nusimovici, M.A., (1975) Phys. Stat. Sol. (b) 79, 229.  
 [46]. Hass M. and Hennis B. W. J., (1962) Phys. Chem. Sol. 23, 1099.  
 [47]. Slater J.C. and Kirkwood J.G., (1931) Phys. Rev. 37, 682.  
 [48]. Lee B.H.J. Appl., (1970) Phys. 41, 2988.  
 [49]. Rajput B.D. and Browne D. A., (1996) Phys. Rev. B 53, 9052.  
 [50]. Smart C., Wilkinson G.R. and Karo A.M., (1965) Lattice Dynamics, edited by Wallis R.F.  
 [51]. Sadao Adachi; Semiconductor Wiley series in materials for Electronic and opto electronic Application. Department of Electric Engineering Gunma University Japan (1956)  
 [52]. Gerlich, D. and Wolf, M., (1980) High pressure Sci. Technol. 1, 506.  
 [53]. Ford P.J., Miller A.J., Saunder G.A., Yogurteu Y.K., Furdyana J. K. and Jeezynski M.J., (1982) Sol. Stat. Phys. (C) 15, 657.  
 [54]. Soma, T., Kagaya, H. M.: (1983) Phys. Status Solidi (b) 118, 245.  
 [55]. Peresada G.L., (1972) Soviet, Phys. Sol. Stat. 14, 1546.  
 [56]. S.R.B thapa, Indian Journal of research (2011) 5, 47-54.

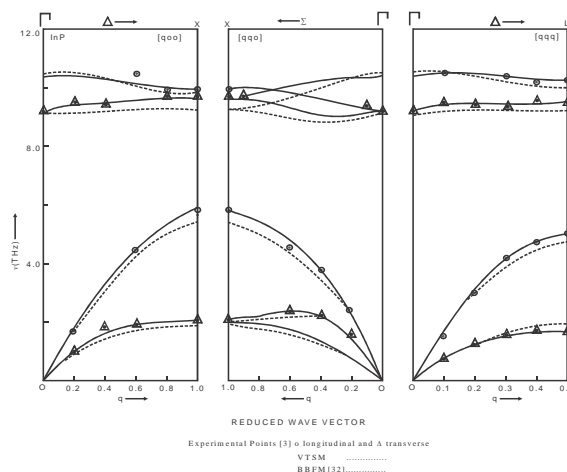


Fig. 1 : Phonon dispersion curves for InP

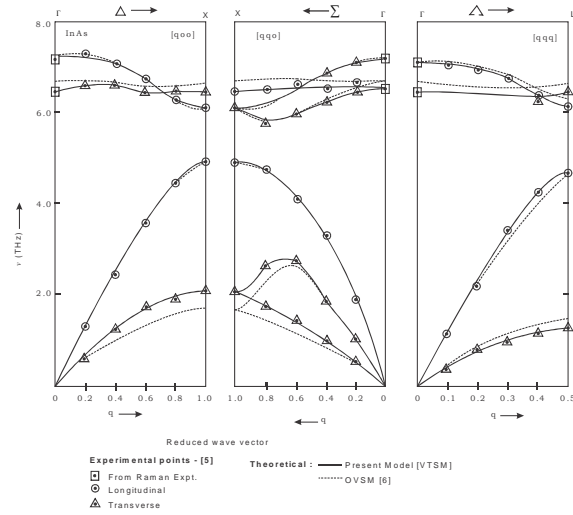


Fig. 2 : Phonon dispersion curves for InAs.

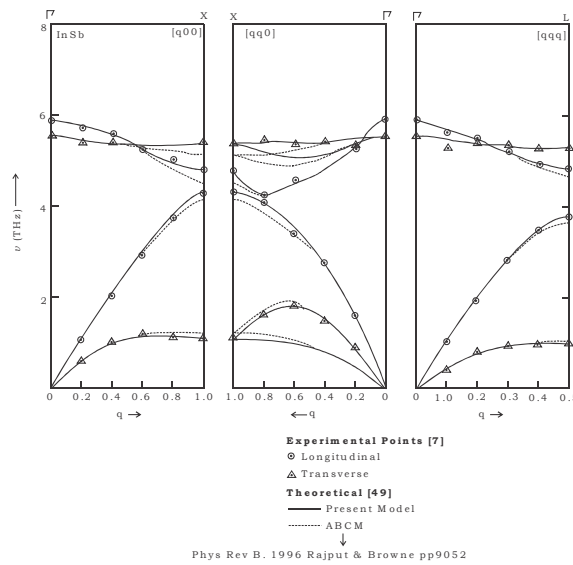


Fig. 3 : Phonon dispersion Curves for InSb

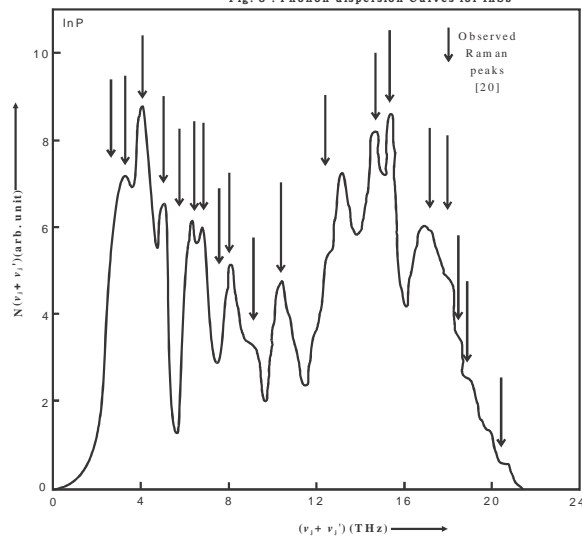


Fig. 4 : Combined density of states curve for InP



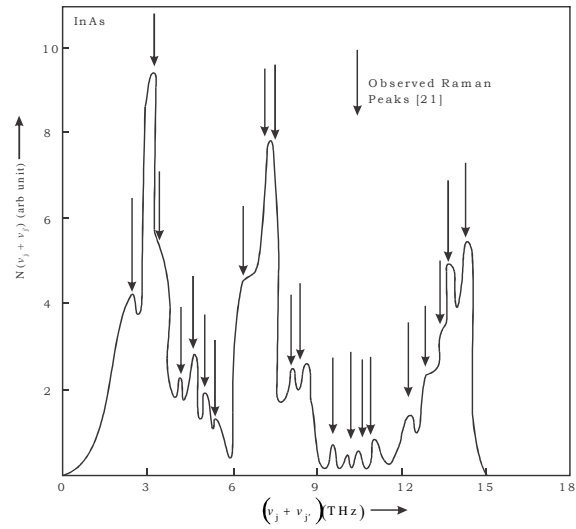


Fig. 5 : Combined density of states curve for InAs

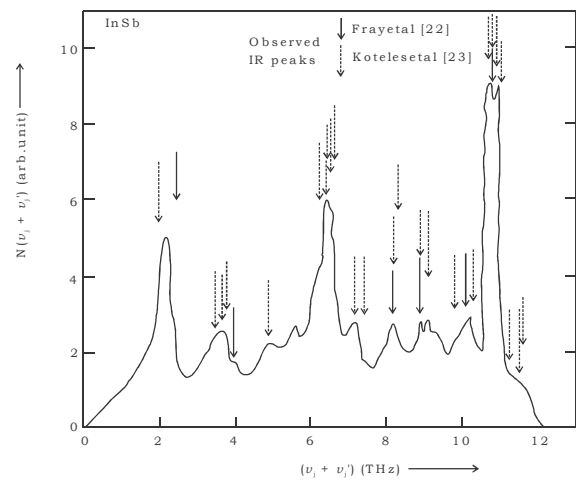


Fig. 6 : Combined density of States curve for InSb

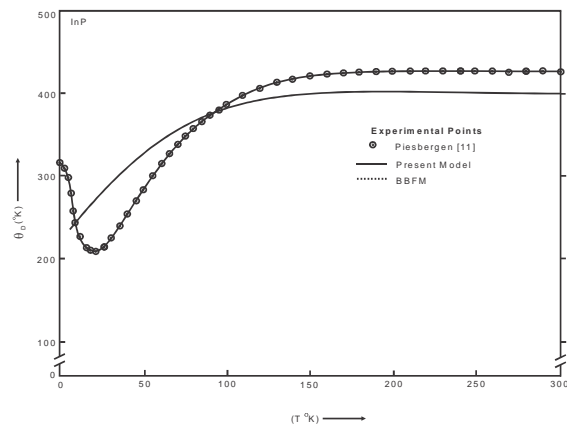


Fig. 7 : Debye temperature variation of InP

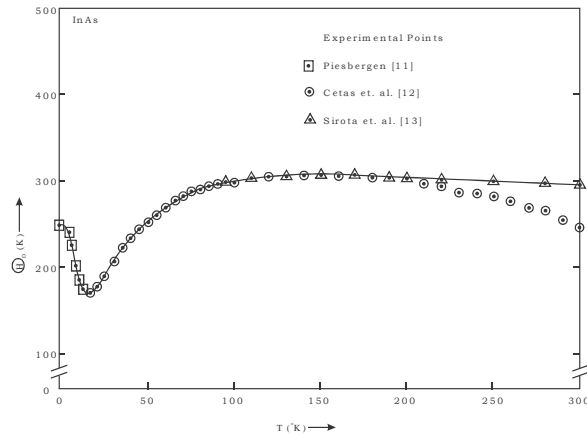


Fig. 8 : Debye characteristic temperature  $\theta_D$  (°K) as a function of temperature T for InAs

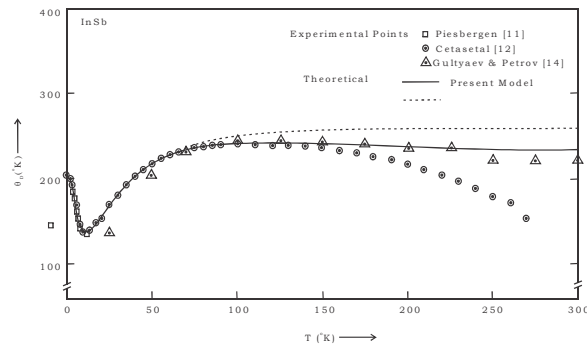


Fig. 9 : Debye temperature variation of InSb

Ref. :  
 (11) U. Piesbergen, Semiconductor and Semimetal 349(1966)  
 (12) T.C. Cetasa, C.R. Tilford, and C.A. Swenson, Phys. Rev. 174, 835(1968)  
 (14) P.V. Gulyaev and A.V. Petrov, Sov. Phys. Solidstate, 1, 330(1959)  
 (15) R. Banerjee and Y.P. Varshni, Canadian Journal of Physics, 47, 451(1969)  
 (16) S.R. Passler, AIP Advances 3, 082108(2013)

**Table- 1:** Input Data and Model Parameter for InP, InAs, InSb  $C_{ij}$  and B (in  $10^{11}$  dyne/cm<sup>2</sup>),  $\nu$  in (THz),  $r_0$  (in  $10^{-8}$  cm)  $\alpha_i$  (in  $10^{-24}$  cm<sup>3</sup>),  $b$  (in  $10^{-12}$  erg),  $\rho$  (in  $10^{-8}$  cm)

Properties	Input Data			Model Parameters			
	InP	InAs	InSb	Parameter	InP	InAs	InSb
$C_{11}$	10.22 <sup>a</sup>	8.329 <sup>c</sup>	6.67 <sup>l</sup>	b	1.05	1.47	1.79
$C_{12}$	5.76 <sup>a</sup>	4.526 <sup>c</sup>	3.65 <sup>l</sup>	$\rho$	0.341	0.56	0.576
$C_{44}$	4.60 <sup>a</sup>	3.959 <sup>c</sup>	3.02 <sup>l</sup>	$f(r_0)$	-0.28	-0.26	-0.26
B	7.25 <sup>b</sup>	-5.79 <sup>d</sup>	4.51 <sup>l</sup>	$r_0 f'(r_0)$	0.111	1.2117	1.263
$r_0$	2.54 <sup>a</sup>	2.61 <sup>c</sup>	2.80 <sup>l</sup>	$A_{12}$	3.068	12.71	15.199
$\nu_{LO}(\Gamma)$	10.46 <sup>*</sup>	7.38 <sup>h</sup>	5.90 <sup>d</sup>	$B_{12}$	-16.209	-6.78	-8.052
$\nu_{TO}(\Gamma)$	9.20 <sup>b</sup>	6.63 <sup>h</sup>	5.54 <sup>d</sup>	$A_{11}$	41.598	58.51	50.731
$\nu_{LO}(L)$	10.20 <sup>b</sup>	6.89 <sup>h</sup>	5.38 <sup>d</sup>	$B_{11}$	-5.3672	-26.18	-12.341
$\nu_{TO}(L)$	9.5 <sup>b</sup>	6.47 <sup>h</sup>	1.12 <sup>d</sup>	$A_{22}$	-5.722	20.52	-8.434
$\nu_{LA}(L)$	5.0 <sup>b</sup>	4.69 <sup>h</sup>	4.82 <sup>d</sup>	$B_{22}$	-3.656	-14.27	-42.125
$\nu_{TA}(L)$	1.65 <sup>b</sup>	1.27 <sup>h</sup>	3.81 <sup>d</sup>	$d_1$	0.1237	0.1369	0.2196
$\alpha_1$	0.221 <sup>a</sup>	0.221 <sup>f</sup>	0.221 <sup>a</sup>	$d_2$	3.5245	2.8569	3.8436
$\alpha_2$	6.8449 <sup>a</sup>	7.50 <sup>g</sup>	13.2519 <sup>a</sup>	$y_1$	-1.1615	-0.7152	-0.4769
$\epsilon_0$	12.40 <sup>a</sup>	12.3 <sup>c</sup>	17.88 <sup>k</sup>	$y_2$	-1.2626	-2.1456	-1.6331
$\epsilon_\infty$	9.61 <sup>a</sup>	15.15 <sup>c</sup>	-	-	-	-	-

**Ref.:**

- (a) K.Kunc etal. phys.stat.vol. (b) 72, 229, (1975) [37]
- \* Extrapolated
- (b) PH Borchers, GF Alfrey, DH saunderson and ADB woods Solid state physics vol. 8.1975. [3]
- (c) Gray, D.W. (1972), American Institute of Physics hand book. 3<sup>rd</sup> ed. [38]
- (d) Price D.L., Row J.M. and nicklow R.M., Phys. Rev. B3, 1268 (1971) [7]
- (e) Levinstein M, Rumyant sev S and shur M 1990 Hand Book series on Semiconductor Parameters Vol 1, 2 (London : World Scientific) [40]
- (f) Kushwaha M.S. & S.S. Kushwaha, (and J. Phys. 58, 351 (1980) [39]
- (g) Shanker etal. 1977 [42]
- (h) Carles, R., Saint-Cnq, N., Renucci, J.B., Renucci, M.A. Zwik, A. : Phys. Rev. B22 (1980) 4804 [5]
- (i) J slutsky and c.w. Garland, Phys. Rev. 113, 167 (1959) [43]

- (j) R. Banerjee and Y.P. Varshni *Canad. J Phys.* 47, 451 (1969) [44]  
 (k) M. Hass and B.W. Hennis *J. Phys. Chem. Solids* 23, 1099 (1962) [46]

**Table-2 :** Vander Waal's Interaction Coefficient for InP, InAs, InSb  $C_{ij}$  and C in unit  $10^{-60}$  erg  $\text{cm}^6$  and  $d_{ij}$  and D in unit  $10^{-76}$  erg  $\text{cm}^8$

Parameter	Inp	InAs	InSb
$C_{+-}$	494	671	956
$C_{++}$	372	401	431
$C_{--}$	721	1208	2286
$d_{+-}$	387	490	748
$d_{++}$	189	205	227
$d_{--}$	704	1077	2067
C	2569	3535	5200
D	1690	2160	3341

**Table-3 :** Assignment for the observed peak positions in Combined Density of States in terms of selected phonon frequencies at  $\Gamma$ , X and L critical points for InP

CDS Peaks ( $\text{cm}^{-1}$ )	Raman Active		
	Observed Raman Peaks ( $\text{cm}^{-1}$ ) [20]	Present Study	
		Values $\text{cm}^{-1}$	Assignments
.....	85	87	LA-TA( $\Delta$ )
107	107	110 110	2TA(L) LA-TA(L)
133	135	136	2TA(X)
163	163	170	TO-LA( $\Delta$ )
.....	189	190	LO-LA( $\Delta$ )
213	214	213	LA-TA( $\Delta$ )
227	228	220	LA+TA (L)
.....	251	257	LO-LA(L)
268	269	263	LA+TA(X)
305	304	300	2LA( $\Delta$ )
343	346	.....	.....
410	412	.....	.....
492	490	490	LO+LA( $\Delta$ )
513	510	517	LO+LA(X)
573	573	.....	.....
593	596	.....	.....
.....	620	614	2TO( $\Gamma$ )
630	626	634	2LO(L)
683	684	680	2LO( $\Delta$ )

**Table- 4 :** Assignment for the observed peak positions in Combined Density of States in terms of selected phonon frequencies at  $\Gamma$ , X and L critical points for InAs

C.D.S. Peaks ( $\text{cm}^{-1}$ )	Raman Active		
	Observed Raman Peaks ( $\text{cm}^{-1}$ ) [6, 21]	Present Study	
		Values ( $\text{cm}^{-1}$ )	Assignment
88	87.5	86	2TA (L)
108	106.5	107	LO-LA ( $\Delta$ )
115	112	114	LA-TA (L)
142	143	136	2TA (X)
154	157	158	TO-TA ( $\Delta$ )
167	165	168	LO-TA ( $\Delta$ )
177	176	175	LA+TA ( $\Delta$ )
220	217.3	200	LA + TA (L)
240	238.6	236	2LA ( $\Delta$ )
.....	253	.....	.....
272	270	271	LO + TA (X)
279	279	282	LO + TA ( $\Delta$ )
328	320	314	2LA (L)
338	343	343	LO + LA ( $\Delta$ )
350	356	.....	.....
367	365	368	LO + LA (X)
410	409	406	{ 2LO (X) 2LO (L)
434	432	433	{ 2TO (X) 2TO (L)
443	445	444	2TO ( $\Gamma$ )
455	456.5	450	2 LO ( $\Delta$ )
482	479	494	2LO ( $\Gamma$ )

**Table- 5:** Assignments for the observed peak positions in Combined Density of States in terms of selected phonon frequencies at  $\Gamma$ , X and L critical points for InSb

CDS Peaks ( $\text{cm}^{-1}$ )	I.R. Active			
	Observed I.R. Peaks		Present Study	
	Exp. [22]	[23]	Value ( $\text{cm}^{-1}$ )	Assignment
73	82.6	–	80	2TA ( $\Delta$ )
87	84 – 87	86	80	2TA ( $\Delta$ )
–	115	–	–	–
–	117	–	–	–
134	124	134	137	LA + TA ( $\Delta$ )
–	127	–	–	–
163	161	–	–	–
190	–	–	193	2LA ( $\Delta$ )
205	208	–	–	–
212	211	–	–	–
–	214	–	213	TO + TA (L)
–	214	–	213	TO + TA ( $\Delta$ )
218	219	–	217	LO + TA (L)
–	220	–	–	–
–	225	–	–	–
240	240	–	–	–
–	246	–	–	–
–	–	–	267	TO + LA (L)
270	–	–	270	TO + LA ( $\Delta$ )
–	–	–	–	LO + LA (L)
–	273	274	273	LO + LA ( $\Delta$ )
–	278	–	–	–
296	299	297	–	–
301	305	–	–	–
–	320	–	–	–
–	322	–	–	–
–	326	–	–	–
338	–	336	–	–
–	345	–	346	2TO ( $\Delta$ )
–	349	–	350	LO + TO ( $\Delta$ )
357	356	–	353	2LO ( $\Delta$ )
–	359	361	–	–
–	363	–	–	–
–	367	–	–	–
–	370	–	–	–
–	375	–	–	–
–	384-388	–	–	–

**Table- 6 :** Third Order Elastic Constant (in the unit  $10^{12}$  dyne/cm<sup>2</sup>) for InP, InAs, InSb

Crystals	$C_{111}$	$C_{112}$	$C_{123}$	$C_{144}$	$C_{166}$	$C_{456}$	Ref.
InP	-9.216	-2.346	-5.927	-7.927	+2.16	0.1325	Present Study
	-8.60	-1.85	-5.1	-6.5	+1.6	-0.042	Other Theoretical results [51]
InAs	-5.373	-2.272	-1.790	-1.706	-0.940	-0.190	Present Study
	-3.56	-2.66	-1.00	+0.16	-1.39	-0.004	Other Theoretical results [51]
InSb	-4.79	-2.547	+0.416	+0.742	-3.241	-1.246	Present Study
	-3.56	-2.66	-1.00	0.16	-1.39	-0.004	Other Theoretical results [51]

**Table-7:** Values of pressure derivatives of SOEC(in dimensionless)for InP,InAs,InSb

Crystals	$Dk/dp$	$ds'/dp$	$dc_{44}/dp$	Ref.
InP	5.2	-0.233	0.80	Present Study
	4.88	-0.29	0.26	Experimental [52]
	4.50	-0.89	0.79	Other [53]
InAs	3.74	0.80	2.08	Present Study
	2.79	0.78	0.56	Experimental [54]
	3.40	0.67	0.46	Other [53]
InSb	3.94	0.53	0.42	Present Study
	4.58	0.47	0.47	Experimental [55]
	4.19	1.23	1.23	Other [53]

**Table- 8 :(X and L Points):** Comparison of Frequencies from Various Source for InP

Point	Branches	Expt. [3]	BBFM [37]			VTSM (Present Study)			% Improvement (a ~ b)
			Value	± Deviation	% (a)	Value	± Deviation	% (b)	
X 100	L <sub>O</sub> (THz)	9.95	9.74	0.21	2.11	10.0	0.05	0.50	1.61
	T <sub>O</sub> (THz)	9.70	9.22	0.43	4.43	9.65	0.05	0.86	7.24
	L <sub>A</sub> (THz)	5.8	5.33	0.47	8.10	5.85	0.05	0.86	7.24
	T <sub>A</sub> (THz)	2.05	1.85	0.20	9.76	2.05	0.00	0	9.76
L (.5 .5 .5)	L <sub>O</sub> (THz)	10.2	9.99	0.03	0.29	10.15	0.05	0.49	0.20
	T <sub>O</sub> (THz)	9.5	9.22	0.28	2.95	9.5	0.00	00	2.95
	L <sub>A</sub> (THz)	5.0	4.72	0.18	3.6	4.95	0.05	1	2.6
	T <sub>A</sub> (THz)	1.65	2.00	0.35	21.21	1.65	0.00	0	21.21

**Table- 9 :** (X and L points) : Comparison of Frequencies from Various Sources of InAs

Point	Branches	Expt. [5] (THz)	OVSM [6]			Present			% Improvement (a ~ b)
			Value (THz)	± Deviation	% (a)	Value	± Deviation	% (b)	
X (100)	LO	6.09	6.09	0.00	0.0	6.10	.01	0.16	0.16
	TO	6.47	6.69	0.22	3.40	6.50	.03	0.46	2.94
	LA	4.95	4.95	0.00	00	4.95	0.00	00	00
	TA	2.03	1.65	0.38	18.7	2.05	.02	0.98	17.72
L (0.5, 0.5, 0.5)	LO	6.09	6.39	0.30	4.92	6.10	.01	0.16	4.76
	TO	6.47	6.66	0.19	2.94	6.50	.03	0.46	2.48
	LA	4.69	4.53	0.16	3.41	4.7	.01	0.21	3.2
	TA	1.27	1.47	0.20	15.75	1.30	.03	2.36	13.39

**Table- 10 :** Comparison of Frequencies from Various Sources (X, L and Δ points) for InSb

	Branches	Expt. [7]	ABCM [49]			VTSM (Present Study)			% Improvement (a ~ b)
			Value	± Deviation	% (a)	Value	± Deviation	% (b)	
X 100	LO	4.75	4.5	0.25	5.26	4.75	0.00	0.00	5.26
	TO	5.38	5.15	0.23	4.27	5.30	0.08	1.49	2.98
	LA	4.30	4.25	0.05	1.16	4.30	0.00	0.0	1.16
	TA	1.12	1.20	0.08	7.14	1.10	0.02	1.78	5.36
L (0.5, 0.5, 0.5)	LO	4.82	4.70	0.12	2.49	4.85	0.03	0.62	1.87
	TO	5.31	5.30	0.01	0.19	5.30	0.01	0.19	0.00
	LA	3.81	3.65	0.16	4.20	3.80	0.01	0.26	3.94
	TA	0.98	1.05	0.07	7.14	1.00	0.02	2.04	5.1
Δ (0.6, 0, 0)	LO	5.28	5.25	0.05	0.95	5.3	0.02	0.38	0.57
	TO	–	5.15	–	–	5.20	–	–	–
	LA	2.90	2.85	0.05	1.72	2.90	0.00	0.00	1.72
	TA	1.20	1.20	0.00	0.00	1.20	0.00	0.00	0.00

IOSR Journal of Applied Physics (IOSR-JAP) is UGC approved Journal with Sl. No. 5010, Journal no. 49054.

Suresh Chandra Pandey. “Lattice Dynamical Study of Indium Pnictides (In P, InAs, InSb).” IOSR Journal of Applied Physics (IOSR-JAP), vol. 9, no. 5, 2017, pp. 01–13.